International Journal of Engineering Research & Technology (IJERT)
ISSN: 2278-0181
Vol. 12 Issue 01, January-2023

Synthesis And Investigation of Cobalt Ferrite Nanoparticles: Structural, Morphological, Optical, Magnetic, and Dielectric Properties

D.Chinna Venkata Subbaiah[1], S Dastagiri[2], G.Pakardin[3*], G. Md. Dastageer[4], M.V. Lakshmaiah[2*]
[1] Department of Physics, Yogi Vemana University, YSR Kadapa, A.P., India.
[2] Department of Physics, Sri Krishnadevaraya University, Ananthapuramu, A.P., India.
[3]Department of Physics, SCNR Govt. Degree College, Proddatur, YSR Kadapa, A.P., India.
[4] III B.Tech (EEE), Amrita Vishwa Vidyapeetham, Bengaluru, K.A., India.

Abstract:- **Cobalt ferrite nanoparticles were synthesized by using a low-temperature hydrothermal method. The structural, optical, Photo luminousness, morphology, elemental composition, magnetization, and electrical properties of cobalt ferrite nanoparticles were carried by XRD, PL, UV-VIS, FT-IR, FE-SEM, EDX, VSM, and LCR techniques, respectively. The XRD pattern exhibited the single-phase cubic spinel structure. The PL studies reveal that the excitation wavelength is at 430 nm, which attribute to the recombination of electrons and holes. The presence of peaks of respective elements (Co, Fe, and O) in the EDX spectrum showed the formation of $CoFe_2O_4$. The UV- Visible Spectrophotometer was estimated by the direct energy band gap of Cobalt ferrite nanoparticles. The magnetic parameters were estimated by VSM. The FT-IR Spectra of the formation of the ferrite have been phase confirmed. The frequency variation of dielectric parameters such as dielectric constant and loss, and ac-conductivity measurements were done along the difference with room temperature and frequency was described.**

Keywords:- Low-temperature hydrothermal method, magnetization, nanoparticles, direct energy band gap

1. INTRODUCTION

Along with diverse types of nanomaterials, magnetic nanoparticles (MNPs) have remunerated human intellect by illustrating amazing attention owing to their technological and biological applications in multifarious acreage [1-3], to their appealing structural, magnetic, and electrical properties. The Spinel ferrites with a common formula of MFe_2O_4, (M: Fe, Mn, Co, Ni, Cu, Zn, etc.) are a large group of this family, which have attracted attention due to their excellent magnetic and electrical properties alongside their semiconducting properties [4–6]. Cobalt ferrite ($CoFe_2O_4$) nanoparticles as an interesting member of these materials have remarkable features such as excellent chemical stability, high coercivity, strong anisotropy, and great saturation magnetization [7]. Curie temperature is one of the important parameters for every ferrite in scintillating to its intrinsic property that could with precision control by the preferential preparation conditions, etc. Bulk $CoFe_2O_4$ is a ferromagnetic material with a Curie temperature T_C of 350 ^oC [8].

The privilege ways to synthesize $CoFe_2O_4$ nanoparticles are many such as the micro-emulsion technique [9], electrospinning [10], ball milling [11], combustion method [12], co-precipitation route [13], a hydrothermal method [14] sol-gel [15], etc. The hydrothermal method is one of the cans techniques to prepare spinel-structured ferrite nanoparticles at low temperatures. It offers a reward in remaining than other techniques such as controlled crystallite size, high transparency, no agglomeration of the particles, and altering the particle surface along with homogeneity [16, 17]. This manuscript elucidates the preparation of uniform-sized cobalt ferrite nanoparticles by hydrothermal method and their properties were investigated.

2. EXPERIMENTAL

The initial materials were preferred as Co $(NO_3)_2$ $6H_2O$ and Fe $(NO_3)_3$ $9H_2O$ (each of 99.9% purity, Sigma-Aldrich) to synthesize the Cobalt ferrite (CF) nanoparticles. Upon taking their stoichiometric scale, these precursors were combined. Moving to a glass beaker was the whole combined precursor. In addition, purified water in the ratio of 1:4 (mixed precursors (gm): distilled water (ml)) is applied to the precursors and the resultant solution is placed on a magnetic stirrer. To swirl the water, this 500 rpm stirring intensity (shown in Fig.1) is retained. NaOH solution will be applied gradually and the pH value will be 12. This solution is transferred in an autoclave to a 300 ml Teflon tube. At an operating temperature of 150º C/8 hours, the enclosed autoclave is placed in a hot-air oven. The autoclave was gradually cooled to room temperature after the reaction had been finished. The final Cobalt ferrite (CF) nanoparticles were extracted from the autoclave coated with Teflon and washed 10 to 12 times with acetone and distilled water until the pH was decreased to 7. Finally, CF nanoparticle samples characterized by XRD, PL, EDX, FE-SEM, UV-VIS, FT-IR, VSM, and LCR techniques for structural, Photo luminousness, elemental composition, morphology, optical, magnetization, and electrical properties of cobalt ferrite nanoparticles.

International Journal of Engineering Research & Technology (IJERT)
ISSN: 2278-0181
Vol. 12 Issue 01, January-2023

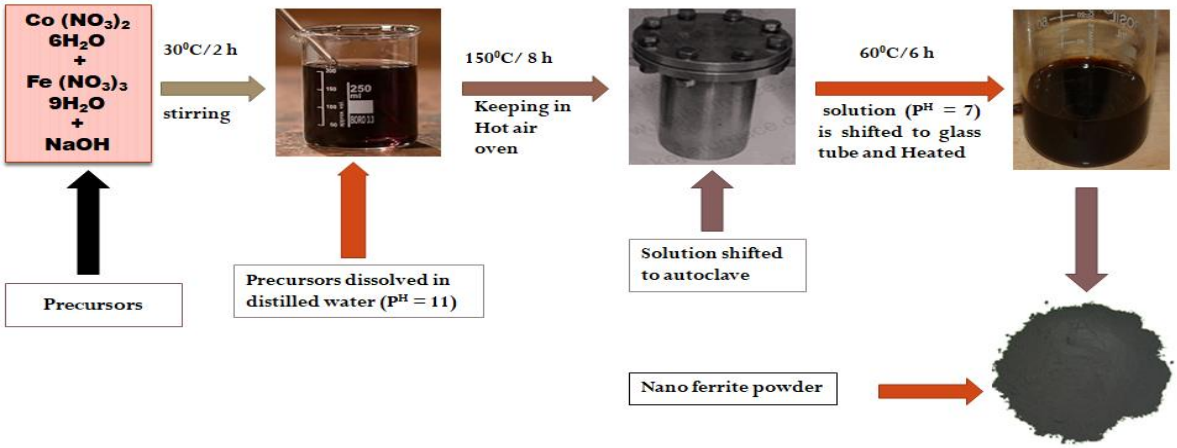

Fig.1. Experimental part of Cobalt ferrite nanoparticles

3. RESULTS AND DISCUSSIONS

3.1. XRD Analysis

Fig.2. shows the X-ray diffraction (XRD) patterns of the Cobalt ferrite (CF) nanoparticles prepared via the hydrothermal method. The XRD patterns were confirmed (JCPDS Number 22-1086). The diffraction peaks of the synthesized Cobalts ferrite nanoparticles corresponding to the (220), (311), (400), (422), (511), and (440) was single spinel phase [18]. The position (2Θ) of the XRD peaks and their full-width half maxima (FWHM) are used to estimated the lattice parameter with the following equation [19]

$$a = 2\lambda \, Sin\, \Theta \, (h^2+k^2+l^2)^{1/2} \text{ ------- (1)}$$

where 'a' is the lattice parameter, Θ is the diffraction angle, λ is the wavelength of the X-ray and h, k, l, are miller indices of each plane family.

The crystallite size of the Cobalt ferrite nanoparticles was calculated by using Debye- Scherrer's equation [20]

$$D_a = \frac{k\lambda}{\beta \, Cos\, \theta} \text{ ------- (2)}$$

The evaluation of theoretical ρ_x, ρ_b, and Porosity (P) were done by using equation [21, 22]

$$\text{X-ray density } (\rho_x) = \frac{8Mw}{NV} \text{ ------- (3)}$$

where V is Unit cell Volume = a^3 (for a = b = c and α = β = γ = 90º), N = Avogadro number (6.023 x 10^{23}), and Mw is molecular weight of cobalt ferrite nanoparticles.

The bulk density (ρ_b) was estimated by the ratio of mass (M) and bulk volume (V= $\Pi r^2 h$) of the Cobalt ferrite nanoparticles pellets, by using equation

$$\rho_b = M/ \Pi r^2 h \text{ ------- (4)}$$

Further, the porosity of the Cobalt ferrite nanoparticles was calculated by ρ_x and ρ_b using equation

$$\text{Porosity (P \%)} = [1- (\rho_x / \rho_b)] *100 \text{ --- (5)}$$

Atomic packing factor of cubical spinel structure can be estimated through following formula

$$\text{Atomic Packing Factor} = \frac{1*\frac{4}{3}\Pi\,(\frac{1}{2}a)^2}{a^3} \text{ -- (6)}$$

The Cobalt ferrite nanoparticles were determined dislocation density (ρ), a specific surface area (S) and Specific Surface area to volume ratio were obtained values listed in the Table.1.

Table.1. Data on the XRD structural and physical parameters of Cobalt ferrite (CF) nanoparticles

International Journal of Engineering Research & Technology (IJERT)
ISSN: 2278-0181
Vol. 12 Issue 01, January-2023

Data on XRD analysis of CF nanoparticles

1.	Lattice parameter (a=b=c)	8.313 Aº
2.	Inter-planer spacing (d)	2.047 Aº
3.	FWHM	4.202 (º)
4.	Volume (V)	574.402 $(Aº)^3$
5.	Atomic Packing Factor	0.5214
6.	Crystallite Size (D_a)	4.916 nm
7.	Micro-Strain (ε)	0.0394
8.	D_{W-H}	4.665 nm
9.	ε_{W-H}	0.0598
10.	MW	234.62 g/mol
11.	Dislocation density (ρ)	6.6605E+17
12.	X-Ray density (ρ_x)	5.425 g/cm^3
13.	Bulk density (ρ_b)	4.084 g/cm^3
14.	Porosity % (P)	24.72
15.	Surface Area (S)	224.978 m^2/g
16.	S/V	0.3916

Williamson- Hall Analysis

To estimate the strain and crystallite size, we have preferred the W-H plot for Cobalt ferrite nanoparticles shown in Fig.3 and expressed in equation [23]

$$\mathbf{B\ Cos\Theta = \frac{K\lambda}{D} + 4\varepsilon\ Sin\Theta} \text{ ------- (7)}$$

Where λ= wavelength, β=Full-Width Half Maxima (FWHM), Θ= Bragg's diffraction angle, ε= Micro-strain, and D= crystallite size. The slope of the W-H plot gives the Micro-strain value. The cobalt ferrite nanoparticles Micro-strain (ε_{W-H}) was 0.0598 and the crystallite size (D_{W-H}) calculated was 4.665 nm. The average crystallite sizes estimated by the two methods are close to each other. Further, a good agreement is perceived between the values expressed from the W-H Plot based on Scherrer's formula and the values ε_{W-H} and D_{W-H}. It can be seen in Fig.4 that there is an inverse proportional relationship between the two parameters D & ε [24].

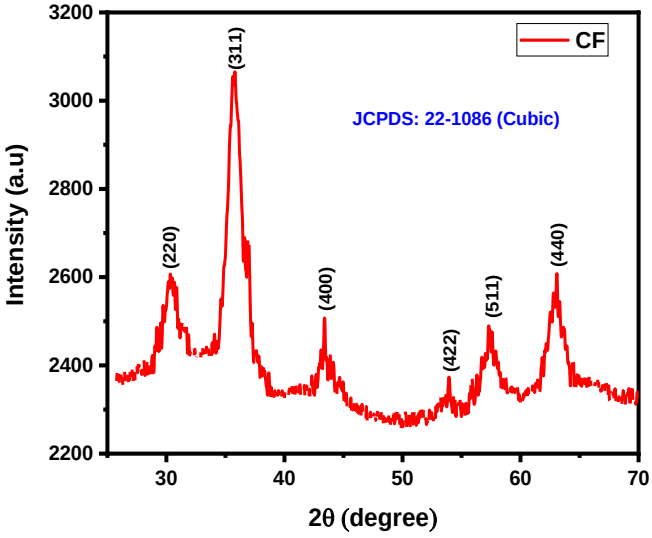

Fig.2. X-ray diffraction (XRD) pattern of Cobalt ferrite nanoparticles

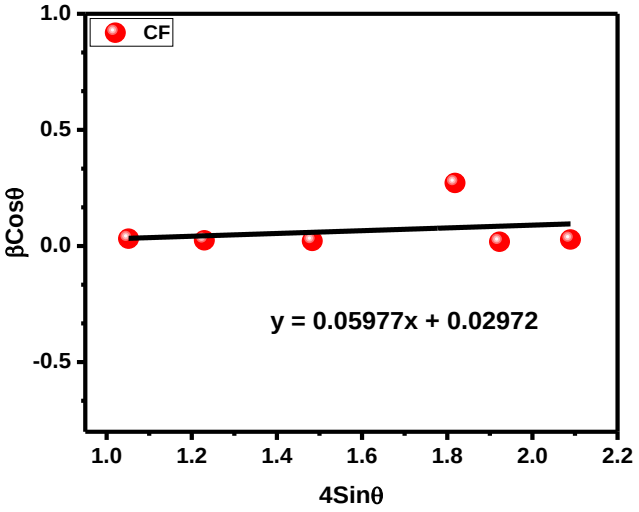

Fig.3. W-H Plot of Cobalt ferrite nanoparticles

3.2. Optical Properties

3.2.1. Photoluminescence Spectral Analysis

The photoluminescence property was studied by a PL spectrophotometer using an excitation wavelength of 216 nm at room temperature. The Fig.5 shows the PL spectra of cobalt ferrite (CF) nanoparticles at room temperature.

International Journal of Engineering Research & Technology (IJERT)
ISSN: 2278-0181
Vol. 12 Issue 01, January-2023

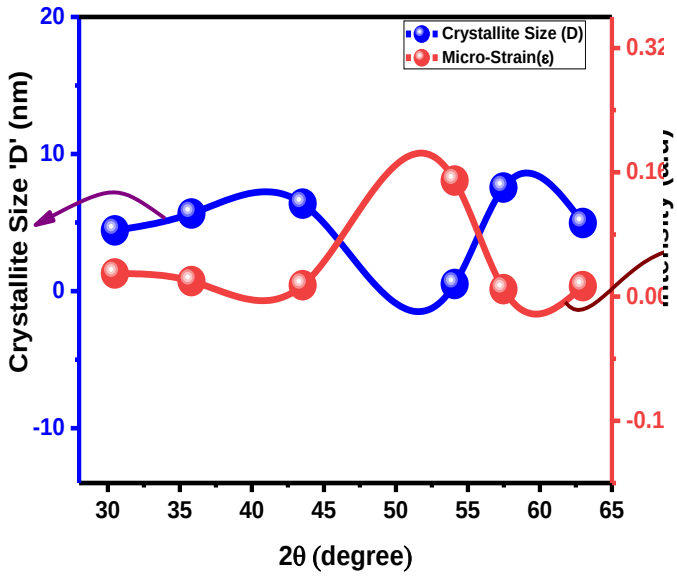

Fig.4. 2Θ values dependence of **D** & **ε** of Cobalt ferrite nanoparticles

The emission peaks were noticed in the visible range of 260 nm to 555 nm, having a maximum near 430 nm. The cobalt ferrite nanoparticles exhibited intense and broad blue emission between 260 nm to 493 nm with peak PL intensity at 430 nm. The emission between 493 nm to 555 nm is related to a weak green emission. Such electronic emission may be due to the radioactive defects at grain boundaries [25, 26] and the oxygen vacancies within the crystal structure [27].

3.2.2. UV-Visible Spectral Analysis

The UV-Visible spectra analysis is one of the optical properties of synthesized Cobalt ferrite nanoparticles were studied. The absorbance in general depends on more than a few factors such as oxygen deficiency, grain size, lattice strain, impurity centers, surface roughness and band gap [28]. The absorption spectra are the maximum absorption wavelength (λ_m) for the Cobalt ferrite nanoparticles that have been observed from shown in Fig.6, it's noticed that λ_m value 295.87 nm.

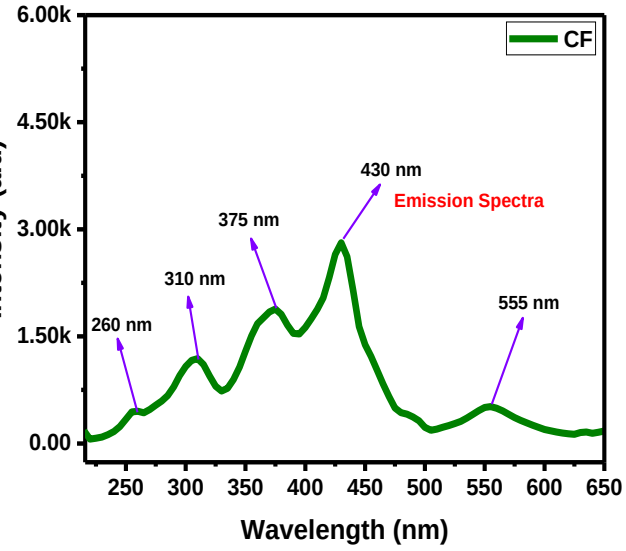

Fig.5. PL pattern of Cobalt ferrite nanoparticles

The optical band gap of spinel ferrite nanopraticles was calculated by using relation,

$$\alpha h\upsilon = A\,(h\upsilon - E_g)^m \quad \text{-------- (8)}$$

where αhυ is the incident photon energy, A is a constant, E_g is the energy band gap of the material, and the exponent m determines the type of electronic transitions, causing the absorption to take a value between ½ and 2. The direct and indirect optical band gap was obtained m=2 and m=1/2, respectively. From shown in Fig.7 observed the direct optical band gap for Cobalt ferrite nanoparticles is found to be 2.38 eV, which is consistent with the previous reports [29] (~2.3 eV). As a result, the Cobalt ferrite nanoparticles can be providing the applications in sensor devices, photocatalytic, and optoelectronic devices [30, 31].

3.2.3. FT-IR Analysis

FT-IR spectra of the cobalt ferrite (CF) nanoparticles at room temperature in a wave number of 400 to 4000 cm^{-1} are presented in Figure. The FT-IR Spectra of Cobalt ferrite nanoparticles is demonstrated in Fig.8, the observed strong broad peak at 537.916 cm^{-1} can be related to the vibration frequency of Fe^{+3} – O. The small peak was at around 396.591 cm^{-1} can be assigned to the vibration frequency of Co^{+2} – O in cobalt ferrite structure. Generally, the two vibrational frequencies were noticed at 537.916 cm^{-1} and 396.591 cm^{-1} were allotted to be tetrahedral and octahedral sites, respectively, for the spinel structure (AB_2O_4). The peaks at 3368.798 cm^{-1} and 1636.912 cm^{-1} can be related to the respective stretching and bending vibrational frequencies of absorbed H_2O on the M-O surface. The peak at 2347.925 cm^{-1} can be due to the CO_2 absorbed on the surface and the peak at 1006.657 cm^{-1} corresponds to the Fe-Co band of prepared Cobalt ferrite nanoparticles [32].

International Journal of Engineering Research & Technology (IJERT)
ISSN: 2278-0181
Vol. 12 Issue 01, January-2023

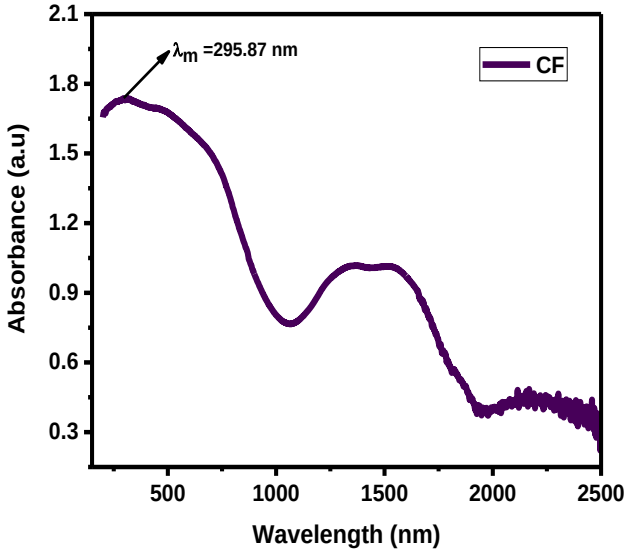

Fig.6. Absorption versus wavelength pattern of Cobalt ferrite nanoparticles

3.3. Magnetic Properties

Magnetic properties of synthesized Cobalt ferrite nanoparticles were characterized by VSM at room temperature with an applied magnetic field 15000 Oe. Fig.9 shows the M-H loop of prepared sample.

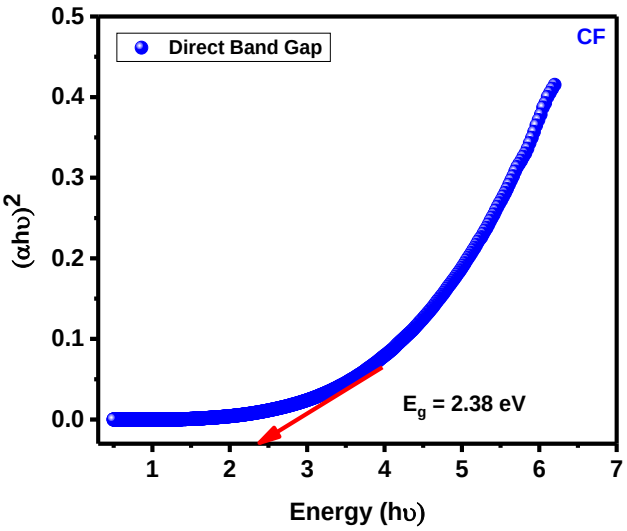

Fig.7. Direct optical band gap of Cobalt ferrite nanoparticles

The values of various magnetic parameter of the Cobalt ferrite nanoparticles such as M_S, M_R, H_C, M_R/M_R ratio, and η_B estimated from the M-H plot was listed in Table.2. The magnetic moment in η_B per formula unit following is computed using the relation

$$\eta_B = \frac{M_S * M_W}{5585} \text{ ------ (9)}$$

Where M_S = Saturation Magnetization and M_W = Molecular weight of the Cobalt ferrite nanoparticles. The magnetic moment η_B was found to be 0.02649.

The magnetic anisotropy (K) is estimated by the following relation [33]

$$K = \{\mu_o * H_C * M_S\}/2 \text{ ------- (10)}$$

Where μ_o is Vacuum permeability, H_C and M_S is Coercivity, Saturation Magnetization, respectively.

The magnetic anisotropy (K) value was 15.5411E-6 erg/cm^3.

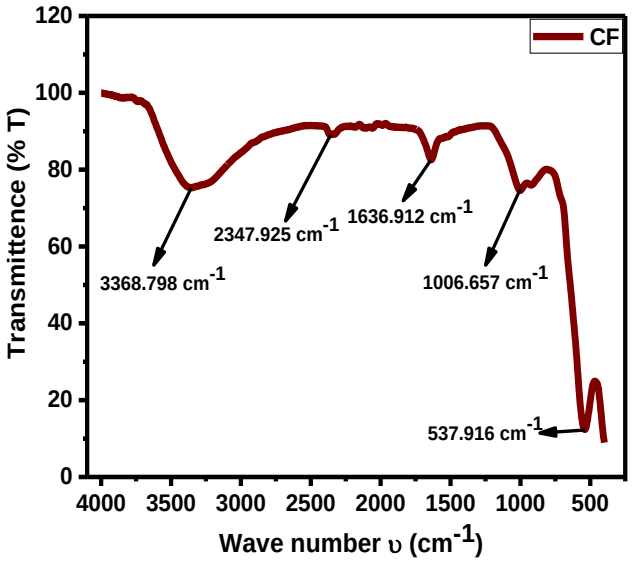

Fig.8. FTIR pattern of Cobalt ferrite nanoparticles

Table.2. Data on the Magnetic parameters of Cobalt ferrite (CF) nanoparticles

Composition	M_S (emu/g)	M_R (emu/g)	H_C (Oe)	M_R/M_S ratio
$CoFe_2O_4$	0.25753	0.01368	96.028	0.05312

3.4. Morphological properties

3.4.1. SEM Analysis

The morphology of prepared Cobalt ferrite nanoparticles was observed by Scanning electron microscopy (SEM). The SEM images show the heterogeneous distribution of agglomerate particles in dense nature, where the shape of the particles are spherical or elliptical and just like stones as shown in Fig.10. The SEM provides that the produced Cobalt ferrite nanoparticles are at micro-range with brisk pores that can be applicable in gas sensors due to its large scale surface area with smaller grain size [34].

International Journal of Engineering Research & Technology (IJERT)
ISSN: 2278-0181
Vol. 12 Issue 01, January-2023

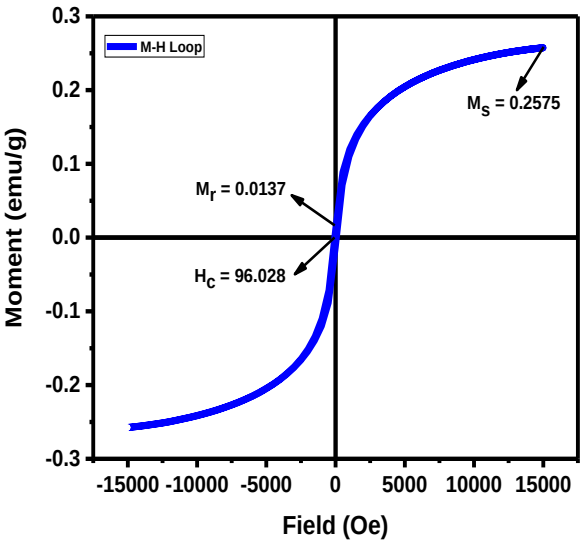

Fig.9. M-H Plot of Cobalt ferrite nanoparticles

The formation of the material can be either amorphous or crystalline, where particles from dense atomic distribution may be affected by spin coupling based on its magnetic behavior [35].

3.4.2. Energy- dispersive X-ray spectroscopy (EDX)

The elemental composition of Cobalt ferrite nanoparticles was carried out by Energy- dispersive X-ray spectroscopy (EDX). Fig.11 shows EDX Spectra for Cobalt ferrite nanoparticles, which indicates the presence of Co, O, and Fe elemental peaks observed in the EDX spectrum which indicated the purity of the cobalt ferrite nanoparticles sample. Elemental compositions of all elements present in the prepared sample were shown in Table 3. This result indicates that the obtained atomic ratio of all elements (Co, O and Fe) was well-matched with the expected stoichiometric proportion of elements in synthesized nanoparticles.

3.5. Dielectric Properties

Dielectric measurement for Cobalt ferrite nanoparticles was carried out at room temperature within the frequency range 100 Hz to 1MHz. In Cobalt ferrite nanoparticles, dielectric constant and loss decreases with increases frequency for the Cobalt ferrite nanoparticles. Dielectric constant and loss decrease sharply at low frequencies and remain almost constant at higher frequencies.

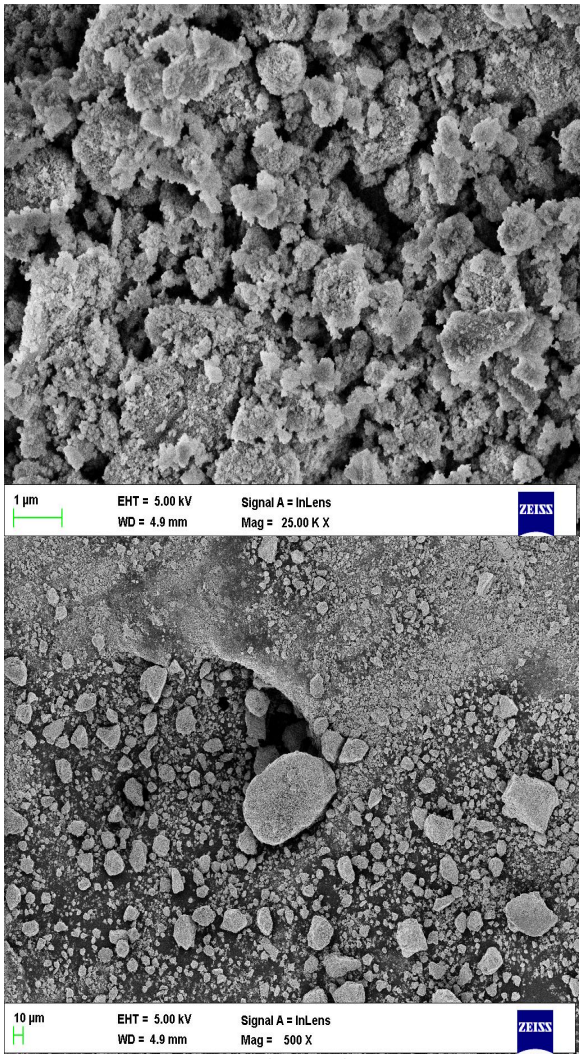

Fig.10. SEM images of Cobalt ferrite nanoparticles

Table.3. Atomic percentage of Cobalt ferrite (CF) nanoparticles

Composition	Atomic Percentage (at %)		
	Co	Fe	O
$CoFe_2O_4$	15.94	26.70	57.36

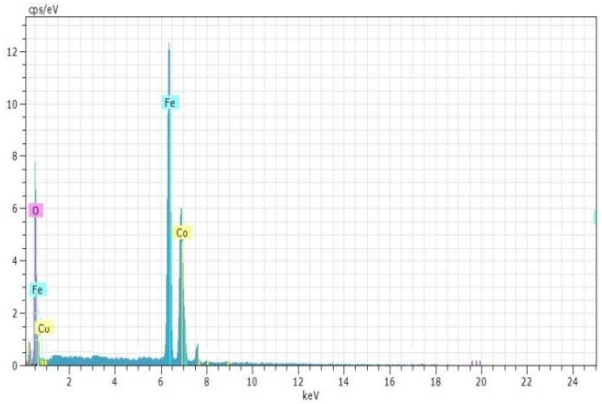

Fig.11. EDX of Cobalt ferrite nanoparticles

This is common trend in spinel ferrite and has been reported in literature by several authors. Variation in dielectric permittivity with frequency can be explained

International Journal of Engineering Research & Technology (IJERT)
ISSN: 2278-0181
Vol. 12 Issue 01, January-2023

based on four forms of polarizations, atomic, electronic, ionic and interfacial [36]. The frequency dependence of dielectric constant (ε') and dielectric loss (ε") of Cobalt ferrite nanoparticles was depicted in Fig.12 & Fig.13. The cobalt ferrite nanoparticles showed the high ε' and ε" values at low log f values. In general, this behavior was attributed to the inhomogeneous dielectric structure. Also, Koop's theory [37] evidenced that the high resistive grain boundaries can be responsible for the high ε' and ε" values at low frequencies. At low log f values, the carriers will be piled up at the grain boundary interface making it high resistive. Thus, the high polarization was developed leading to the high ε' and ε" values. This polarization can be treated as Maxwell-Wagner's interfacial polarization [38]. However, this behavior was not stable. At high log f values, the entire carriers can acquire more energy than the grain boundaries. Therefore, the breakage of grain boundary will be taken place and hence, the carriers will enter the grain portion. This can lead to the high mobility and conductivity of the charges. But the polarization will be decreased indicating the decrease of ε' and ε". From this analysis, it was clear that the grain was responsible for the low ε' and ε" values at high log f. Because of the compositional dependence, the ε' and ε" were observed to be normal in magnitude for Cobalt ferrite nanoparticles. In Fig.14, the log σ_{ac}-log ω plot was shown. This plot indicated that the ac-electrical conductivity (log σ_{ac}) was variation between from 7.066 to 6.655 S/cm corresponding from 100 Hz to 1MHz. This trend was attributed to the thermal activation of the charge carriers. Dielectric constant, dielectric loss and ac-conductivity obtained values were listed in the Table 4. The low-temperature hydrothermal method in comparing to further synthesis methods of nanoparticles preparation has many advantages, for examples: simple, available, and inexpensive. In this work, we have prepared the $CoFe_2O_4$ nanoparticles by low temperature hydrothermal method.

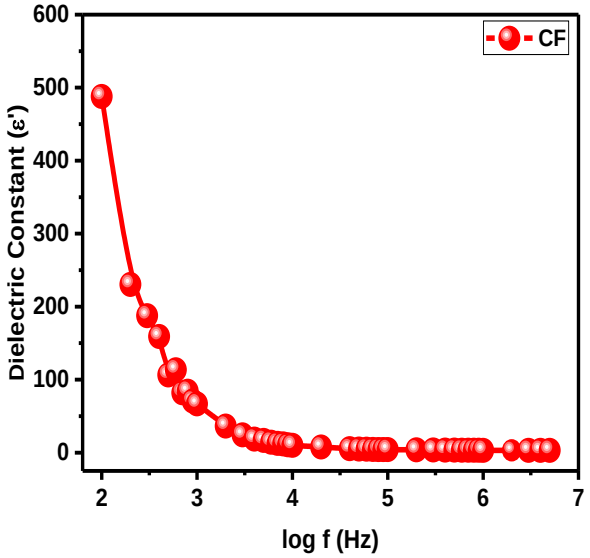

Fig.12. Frequency depends on dielectric constant of Cobalt ferrite nanoparticles

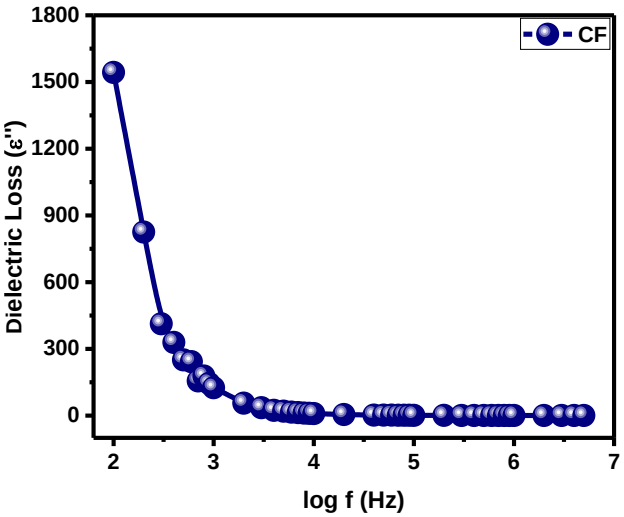

Fig.13. Frequency depends on dielectric loss of Cobalt ferrite nanoparticles

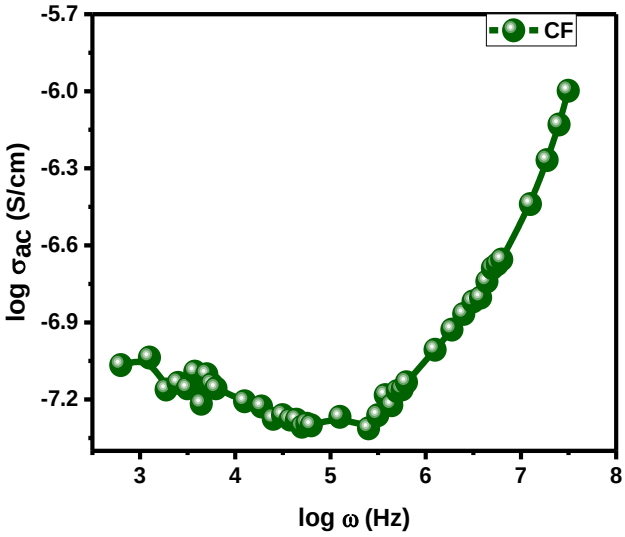

Fig.14. ac-electrical conductivity of Cobalt ferrite nanoparticles

International Journal of Engineering Research & Technology (IJERT)
ISSN: 2278-0181
Vol. 12 Issue 01, January-2023

Table.4. Dielectric parameters of Cobalt ferrite (CF) nanoparticles

S.No.	Frequency (Hz)	Dielectric Constant	Dielectric loss	ac conductivity (S/cm)
1.	100	487.802	1543.007	7.066
2.	1k	66.833	125.278	7.157
3.	10k	10.052	8.989	7.301
4.	0.1M	4.212	1.323	7.133
5.	1M	3.179	0.397	6.655

4. CONCLUSIONS

The low-temperature hydrothermal method in comparing to further synthesis methods of nanoparticles preparation has many advantages, for examples: simple, available, and inexpensive. In this work, we have prepared the $CoFe_2O_4$ nanoparticles by low temperature hydrothermal method. A systematic study on the structural, morphological, optical and dielectric properties of $CoFe_2O_4$ nanoparticles was carried out using various analyses. SEM images reveal with spherical or elliptical and just like stones. The direct optical energy band gap of 2.38 eV, can be providing the applications in photocatalytic, sensor devices, and optoelectronic devices. The magnetic parameters M_S, M_R, H_C, and M_R/M_S values were 0.25753 emu/g, 0.01368 emu/g, 96.028 Oe, and 0.05312, respectively estimated by VSM. The dielectric properties the high dielectric constant (ε') of 487.802, high dielectric loss (ε'') of 1543.007 and ac electrical conductivity (log σ_{ac}) of 7.066 S/cm were recorded at 100Hz were done along with room temperature of Cobalt ferrite nanoparticles.

ACKNOWLEDGEMENTS

The authors express thankfulness to Dr. M.V. Lakshmaiah, Professor (Physics & Electronics), Department of Physics, Sri Krishnadevarya University, Ananthapuramu, for providing Research Lab, My special thanks go to SRMIST consultancy, SRM University, Chennai for providing me the necessary characterizations (XRD, FTIR, and UV-Vis), and SEM with EDAX providing Yogi Vemana University, YSR Kadapa.

REFERENCES:

[1] S.Chang, Q.Haoxue, Tuning Magnetic Properties of Magnetic Recording Media Cobalt Ferrite Nano-Particles by Co-Precipitation Method, IEEE Transactions of magnetics 108 (2009) 1-4.

[2] JR Anusha, Hee Je kim,Albin T.Fleming, S Jerome Das, Kook-Hyun Yu, Simple fabrication of ZnO/Pt/chitosan electrode for enzymatic glucose biosensor, Sensor Actuat B. 202 (2014) ,827-833.

[3] J Emima Jeronsia, L Allwin Joseph, M Mary Jaculin, P Annie Vinosha, S Jerome Das, Hydrothermal synthesis of zinc stannate nanoparticles for antibacterial applications, JTUSCI Doi:10.1016/j.jtusci.2015.12.003**.**

[4] Peredkov, S.; Neeb, M.; Eberhardt, W.; Meyer, J.D.; Tombers, M.; Kampschulte, H.; Niedner-Schatteburg, G. Spin and orbital magnetic moments of free nanoparticles. Phys. Rev. Lett. (2011) 107, 233401.

[5] Salunkhe, A.; Khot, V.M.; Phadatare, M.R.; Pawar, S.H. Combustion synthesis of cobalt ferrite nanoparticles—Influence of fuel to oxidizer ratio. J. Alloys Compd. (2012) 514, 91–96.

[6] Kefeni, K.K.; Msagati, T.A.; Mamba, B.B. Ferrite nanoparticles: Synthesis, characterisation and applications in electronic device. Mater. Sci. Eng. B (2017) 215, 37–55.

[7] Maaz, K.; Mumtaza, A.; Hasanaina, S.K.; Ceylan, A. Synthesis and magnetic properties of cobalt ferrite ($CoFe_2O_4$) nanoparticles prepared by wet chemical route. J. Magn. Magn. Mater. (2007) 308, 289–295.

[8] BD Cullity, CD Graham, Introduction to magnetic materials, John Wiley & Sons.Newjesey (2009).

[9] Huma Malik, Azhar Mahmood, Khalid Mahmood, Maria Yousaf Lodhi, Muhammad Farooq Warsi, Imran Shakir, Hassan Wahab, M. Asghar,Muhammad Azhar Khan, Influence of cobalt substitution on the magnetic properties of zinc nanocrystals synthesized via micro-emulsion route,Ceram.Int,40,(2014), 9439-9444.

[10] Shudan Li, Xianlei Wang,Synthesis of different morphologies lanthanum ferrite ($LaFeO_3$) fibers via electrospinning, Optik, 126 (2015) 408-410.

[11] Yarilyn Cedeno-Mattei, Oscar Perales-Perez, Oswald N.C. Uwakweh, Effect of high- energy ball milling time on structural and magnetic properties of nanocrystalline cobalt ferrite powders, J.Magu.Magn.Mater, 341 (2013) 17-24.

[12] AB Salunkhe, VM Khot, MR Phadatare, SH Pawar, Combustion synthesis of cobalt ferrite nanoparticles - Influence of fuel to oxidizer ratio, J.Alloys comp, 514 (2012) 91-96.

[13] AK Nikumbh, , RA Pawar, DV Nighot, GS Gugale, MD Sangale, MB Khanvilkar, AV Nagawade, Structural, electrical, magnetic and dielectric properties of rare-earth substituted cobalt ferrites nanoparticles synthesized by the co-precipitation method, J.Magu.Magn.Mater,355 (2014) 201-209.

[14] Yüksel Koseoglu, Furkan Alan, Muhammed Tan, Resul Yilgin, Mustafa Ozturk, Low temperature hydrothermal synthesis and characterization of Mn doped cobalt ferrite nanoparticles, Ceram.Int, 38 (2012) 3625-3634.

[15] Tal Meron, Yuri Rosenberg, Yossi Lereah, Gil Markovich, Synthesis and assembly of high-quality cobalt ferrite nanocrystals prepared by a modified sol–gel technique, J.Magu.Magn.Mater,292 (2005) 11-16.

[16] G Fan, Z Gu, L Yang, F Li, Nanocrystalline zinc ferrite photocatalysts formed using the colloid mill and hydrothermal technique,J Chem Eng 155 (2009) 534-541.

[17] CN Chinnasamy, A Narayanasamy, N Ponpandian, K Chattopadhyay, The influence of Fe^{3+} ions at tetrahedral sites on the magnetic properties of nonocrystalline $ZnFe_2O_4$, Mater. Sci. Eng A, 304 (2001) 983-987.

[18] Bradiceanu M, Vlazan P, Novaconi S, Grozescu I, Barvinschi P. Cobalt ferrite nanostructures obtained by chemical coprecipitation and hydrothermal method Chem Bull ”Politehnica” Univ (Timisoara) 52 (2007) 1-2.

[19] M. O’ Donnell et al., Structural analysis of a series of strontium – substituted apatities, Acta Biomater. 4(50 (2008) 1455-1464.

[20] H.Yan, et al., Hao Yan, Jiancheng Zhang, Chenxia You, Zhenwei Song, Benwei Yu, Yue Shen Influences of different synthesis conditions on properties of Fe3O4 nanoparticles , Mater. Chem. Phy. 113 (1) (2009) 46-52.

[21] D. Tomar, P. Jeevannandam, Synthesis of cobalt ferrite nanoparticles with different morphologies via thermal decomposition approach and studies on their magnetic properties, J. Alloys Compd. 843 (2020) 155815.

[22] S. Chakrabarty, A. Dutta, M. Pal, Yttrium doped cobalt ferrite nanoparticles: study of dielectric relaxation and charge carrier dynamics, Ceram. Int. 44 (2018).

International Journal of Engineering Research & Technology (IJERT)
ISSN: 2278-0181
Vol. 12 Issue 01, January-2023

[23] N.Kumar, R.K.Singh, H.K.Satyapal, Structural, Optical and magnetic properties of non-stoichometric lithium substituted magnesium ferrite nanoparticles for multifunctional applications, J. Mater. Sci. Electron. 31 (2020) 9231-9241.

[24] VD Mote, Y Purushotham, and BN Dole, Williamson- Hall analysis in estimation of lattice strain in nanometer-sized ZnO particles, J. Theor. App. Phy, 6;6, (2012) 2251.

[25] C. H. Zang, D. M. Zhang, C.J. Tang, S.J. Fang, Z.J. Zong, Y.X. Yang, C. H. Zhao, Y. S. Zhang, Optical properties of a ZnO/P nanostructure fabricated by a chemical vapor deposition method, J. Phys. Chem. C 113 (2009), 18527.

[26] L.J. Zhuge, X. M Wu,, X. M Yang, Q. Chen, Structural and deep ultraviolet emission of Co-doping ZnO films with Co3O4 nano-clusters, J. Mater. Chem. Phys. 120 (2010)480 – 483.

[27] R. Bhargava, P. K. Sharma, R. K. Dutta, S. Kumar, A.C. Pandey, N. Kumar, Influence of Co-doping on the thermal, structural, and optical properties of sol-gel derived ZnO nanoparticles, J. Mater. Chem. Phys. 120 (2010) 393.

[28] A.S. Ahmed, M. Shafeeq, M. Sinla, S. Tabassum, A.H. Naqvi, A. Azam, Band gap narrowing and fluorescence properties of nickel doped SnO2 nanoparticl;es, J. Lumin. 131 (2011) 1-6.

[29] Sudharshan Vadnala, Nirupam Paul, Amit Agrawal, S. G. Singh, Enhanced infrared sensing properties of Vanadium pentaoxide nanofibers for bolometer application, Mater. Sci, Semicond. Processing 81 (2018) 82-88.

[30] D. Kothandan, R.J. Kumar, M. Prakash, K.C.B. Naidu, Structural, morphological and optical properties of $Ba_{1-x}Cu_xTiO_3$ (x = 0.2, 0.4, 0.6, 0.8) nanoparticles synthesized by hydrothermal method, Mater. Chem. Phys. 215 (2018) 310–315.

[31] C. Srilakshmi, R. Saraf, C. Shivakumara, Structural studies of multifunctional $SrTiO_3$ nanocatalyst synthesized by microwave and oxalate methods: its catalytic application for condensation, hydrogenation, and amination reactions, ACS Omega 3 (2018) 10503–10512.

[32] N.T. To Loan, N.T.Hien Lan, N.T.Thuy Hang, N.Q.Hai, D.T.Tu Anh, Vu Thi Hau, L.V.Tan, T.V.Tran, $CoFe_2O_4$ nanomaterials: effect of annealing temperature on characterization magnetic, photocatalytic, and photo- fanon properties, Processes 7 (2019) 885.

[33] U. B. Sontu, V. Yelasani, V. R. R. Musugu, Structural, electrical and magnetic characteristics of nickel substituted cobalt ferrite nanoparticles synthesized by self combustion method, J. Mag. Magn. Mater. (2015) 374-376.

[34] S.Singh, B. C. Yadav, V. D. Gupta and P. K. Dwivedi, Investigation on effects of surface morphologies on response of LPG sensor based on nanostructured copper ferrite system, Mater. Res. Bull. 47, 11 (2012)

[35] D.Peddis, C. Cannas, A. Musinu and G. Piccaluga, Magnetism in nanoparticles: Beyond the effect of the particle size, Chem. Eur. J. 15, 32 (2009).

[36] A. Verma, R. Chatterjee, Effect of zinc concentration on the structural, electrical and magnetic properties of mixed Mn-Zn and Ni-Zn ferrites synthesized by the citrate precursor technique, J. Magn. Mater. 306(2) (2006 Nov 1) 313-320.

[37] C.G.Koops, On the Dispersion of Resistivity and Dielectric Constant of Some Semiconductors at Audio frequencies, Physical Review 83 (1951) 121-124.

[38] K.W. Wagner, The Distribution of Relaxation Times in Typical Dielectrics, Ann. Phys., 40 (1913) 817.